Article:

Che, K., Tang, D., Ren, C. et al. (4 more authors) (2018) Thermal Characteristics of Brillouin Microsphere Lasers. IEEE Journal of Quantum Electronics , 54 (3). ISSN 0018-9197

https://doi.org/10.1109/JQE.2018.2829986

Thermal Characteristics Of Brillouin Microsphere Lasers

Kaijun Che, Deyu Tang, Changyan Ren, Huiying Xu, Lujian Chen, Chaoyuan Jin, Zhiping Cai

Abstract— **In this paper, we investigate thermal characteristics of Brillouin microsphere lasers theoretically and experimentally. A theoretical model for Brillouin lasing in microcavities is constructed based on couple mode theory. The analytic correlation between Brillouin lasing and thermal power is given. To track the thermal response of Brillouin microlasers, we introduce two kinds of thermal perturbations by either tuning the wavelength of pump wave or varying the surrounding temperature. It is shown that the output power of Brillouin lasers is sensitive to and linearly varied with the thermal change of the mode area and surroundings. The optical bistabilities induced by the resonant transition of the pump wave or Brillouin lasing is further studied and the thermal behavior is well explained by the thermal dynamics of whispering gallery modes. Our results demonstrate that Brillouin microlasers with stable performances hold great potential for sensor applications since thermal or object-induced perturbations on lasing can be simply tracked by the variation of output power.**

***Index Terms*—Thermal characteristics, microsphere, Brillouin microlaser.**

I. Introduction

Brillouin lasing or stimulated Brillouin scattering(SBS) is an coherent nonlinear phenomenon originated from the inelastic scattering of material lattice, where a pump signal wave and the scattered Stokes wave interferes with each other and the mechanical oscillation induced by the electrostriction effect is formed as an acoustic wave at certain frequency[1]-[4]. In the past decades, the SBS has attracted intensive interests for its unique features, such as low threshold and narrow linewidth[4], and been widely developed and investigated in fiber-based system[3], in on-chip photonic circuits[5]-[7] and in whispering gallery mode(WGM) microcavities[8]-[11]. WGM microcavities with high-Q resonances can greatly enhance the light-matter interaction and have become a promising platform for the achievement of low threshold SBS[8]-[18]. Up to date, a variety of cavities have already been employed for SBS, such as silica/tellurite microspheres[10]-[14], silica rods/microbottles/bubbles [15]-[17], and silica/fluoridemm-disks[9][18]-[20]. The SBS can be effectively excited when both pump and scattered Stokes waves are involved into cavity resonances. In addition, some SBS applications, such as microwave synthesizers and filters[21][22], slow light for light storage[23][24], and gyroscopes[25], have been recently

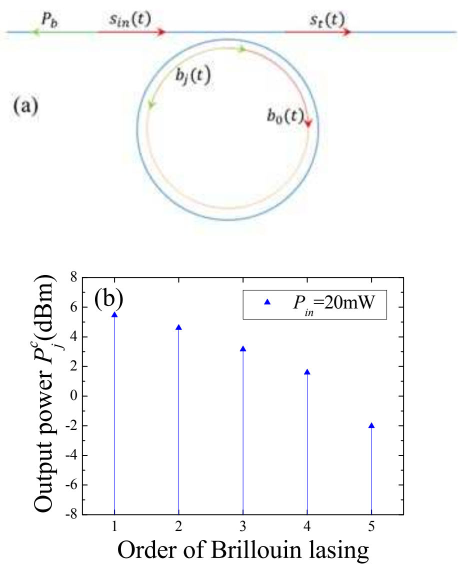

Fig.1. (a) Schematic plot of a taper coupled microcavity; (b) An example of the output power versus the order of cascaded Brillouin lasing when P_{in} = 20mW.

reported. Among all the above mentioned cavities, silica sphere cavities with dimensions of hundreds micrometers possess unique features of ultra-rich mode resonances and easy fabrication[26], which enables the thermal latching of pump wave to WGM resonances fairly easily and is particularly suited for the SBS realization without repeated sweeping of pump wave.

In this work, thermal characteristics of Brillouin silica microsphere lasers are investigated theoretically and experimentally. In section II, we construct a theoretical model for Brillouin lasing in microcavities based on couple mode theory and obtain an analytic correlation between Brillouin lasing and thermal power. In section III, two kinds of thermal perturbations are proposed by either tuning the pump wave or varying the surrounding temperature for the study of thermal responses of Brillouin lasing. In section IV, we perform the experimental investigation by employing the mechanically packaged silica sphere resonator and verify that the lasing output is sensitive to and linearly varied with the resonant shift that is induced by the thermal perturbation. Some lasing behaviors, such as optical bistabilities due to the resonance transition of pump wave or Brillouin lasing, and up to 41.7dB

This work was financially supported by China Scholarship Council (201606315025), and National Science Foundation of China (NSFC) (61107045, 61675172, 61574138). Kaijun Che, Deyu Tang, Changyan Ren, Huiying Xu, Lujian Chen, Zhiping Cai are with Department of Electronic Engineering, Xiamen University, 361005 Fujian, People's Republic of China (e-mail: chekaijun@xmu.edu.cn ; 544921369@qq.com; 924066252@qq.com, xuhy@xmu.edu.cn, lujianchen @xmu.edu.cn, zpcai@xmu.edu.cn).

Chaoyuan Jin is with College of Information Science and Electronic Engineering, Zhejiang University, 310007, Hangzhou, People's Republic of China and Department of Electronic Electric and Engineering, University of Sheffield, Sheffield S3 7HQ, UK(e-mail: jincy@zju.edu.cn).

of side mode suppression ratio (SMSR) are presented. Finally, the conclusions are given in Section V.

II. Theoretical Model Of Brillouin Lasing

Fig. 1(a) shows a schematic plot of Brillouin microsphere lasers. In the theoretical model, we set $s_{in}(t)$ and $s_t(t)$ as amplitudes of incident and transmitted waves in the taper while $P_{in}=|s_{in}(t)|^2$ and $P_t=|s_t(t)|^2$ represent the incident and transmitted pump power. The pump power coupled into cavity P_c is equivalent to $P_{in}-P_t$. $b_0(t)$ and $b_j(t)$ are set as energy amplitudes of the pump wave (regarded as the 0th-order Brillouin lasing) and the j^{th}-order Brillouin lasing as $W_0=|b_0(t)|^2$ and $W_j=|b_j(t)|^2$ represent their energies stored in the microsphere. Based on coupled mode theory[27], similar to a theoretical model for Raman lasing[28], we can construct the following equations to describe the time evolution of $b_j(t)$

$$\begin{cases} \dfrac{\partial b_0}{\partial t}=(i\Delta\omega_0-\kappa_0-g_1^sW_1)b_0+\sqrt{2\kappa_0^c}s_{in} \\ \dfrac{\partial b_j}{\partial t}=(-\kappa_j-g_{j+1}^sW_{j+1}+g_j^sW_{j-1})b_j \\ (j=1,2,...,N-1) \\ \dfrac{\partial b_N}{\partial t}=(-\kappa_N+g_N^sW_{N-1})b_N \end{cases}, \quad (1)$$

where $\Delta\omega_0$ is the detuned angular frequency between pump wave and cavity resonance. $\kappa_j=\kappa_j^i+\kappa_j^c$ is the total field loss rate which comprises of the intrinsic loss rate κ_j^i and the loss rate κ_j^c associated with waveguide coupling. $g_j^s=\Gamma g_0c^2/(2n^2V_{mj})$ is defined as intra-cavity Brillouin gain coefficient, where g_0 is Brillouin gain in bulk silica, n is refractive index, c is the light velocity in vacuum, V_{mj} is mode volume of the j^{th}-order Brillouin lasing coupled WGM, Γ stands for the mode overlap.

For steady state at which the powers or energies of both pump wave and Brillouin lasing in microsphere are invariable, the pump power P_c is dissipated into intrinsic loss and the 1st-order Brillouin lasing power as other power loss routes or nonlinear phenomena are ignored when single or cascaded Brillouin lasing dominates in microsphere:

$$P_c=2(\kappa_0^i+g_1^sW_1)W_0. \quad (2)$$

Additionally, P_c can also be derived from the total power P_{in} used for pumping, namely, the power inserted into taper:

$$P_c=\frac{4\kappa_0^c(\kappa_0^i+g_1^sW_1)}{(\kappa_0+g_1^sW_1)^2+\Delta\omega_0{}^2}P_{in} \quad (3)$$

The power of the j^{th}-order Brillouin lasing $P_j^B=P_j^i+P_j^c+P_{j+1}^B$ includes the intrinsic loss $P_j^i=2\kappa_j^iW_j$, the power $P_j^c=2\kappa_j^cW_j$ coupled out by waveguide and the power $P_{j+1}^B=2g_{j+1}^sW_{j+1}W_j$ as the pump wave for the next order Brillouin lasing. At the same time, P_j^B originates from P_{j-1}^B and $P_j^B=2g_j^sW_jW_{j-1}$. Thus we can obtain the relation between W_{j+1} and W_{j-1}:

$$W_{j-1}=\frac{g_{j+1}^sW_{j+1}+\kappa_j}{g_j^s}. \quad (4)$$

For the last order (N^{th}) lasing, W_{N+1} is 0, $W_{N-1}=\kappa_N/g_N^s$ can be directly obtained and then $W_{j=N-1-2m}$ can be derived from W_{N-1} as $m=1,2,3,...$ from Eq.(4). If N-1-2m=1,we can obtain W_0 from Eq. (2) and Eq.(3), or we can obtain W_1 when N-1-2m=0. Based on the obtained W_0 or W_1, the energies $W_{j=N+2-2m}$ of the other orders Brillouin lasing can be derived from Eq. (4) as well. Finally, the corresponding Brillouin lasing output and intrinsic loss can be obtained:

$$P_j^c=2\kappa_j^cW_j, \quad (5)$$

and

$$P_j^i=2\kappa_j^iW_j, \quad (6)$$

respectively. Fig. 1(b) shows an example of output power for a 5-order cascaded Brillouin lasing, whereas P_{in}=20mW, κ_j^i =0.8π×10^{6}Hz, $\kappa_j^c=4\kappa_j^i$, g_j^s=1.75×10^{14}Hz^2/mW, and $\Delta\omega_0=\kappa_j^i$. One thing should be noted is that the odd and even orders Brillouin lasing propagate in the backward and forward directions, respectively, and here backward Rayleigh scatterings are ignored.

Finally, we can obtain the total intrinsic loss power:

$$P_i=\sum_{j=0}^{N}P_j^i, \quad (7)$$

including both the intrinsic losses of all orders Brillouin lasing and pump wave. We know that most of optical losses induced by the material absorption are transferred into heat, thus P_i can be approximately considered as heat power P_h in microspheres.

For single Brillouin lasing(N=1), the Brillouin lasing output P_1^c and thermal power P_h can be derived as:

$$P_1^c=2\kappa_1^c\sqrt{\frac{2\kappa_0^cP_{in}}{\kappa_1g_1^s}-(\frac{\Delta\omega_0}{g_1^s})^2}-\frac{2\kappa_1^c\kappa_0}{g_1^s} \quad (8)$$

and:

$$P_h=2\kappa_1^i\sqrt{\frac{2\kappa_0^cP_{in}}{\kappa_1g_1^s}-(\frac{\Delta\omega_0}{g_1^s})^2}-\frac{2(\kappa_1^i\kappa_0^c-\kappa_0^i\kappa_1^c)}{g_1^s} \quad (9)$$

As the pump wave is completely coupled with resonances, namely $\Delta\omega_0$=0, P_1^c and P_h reach the maximum values $P_1^c\_m$ and P_h_m, the minimum threshold of single Brillouin lasing can also obtained:

$$P_{in}=\frac{\kappa_1\kappa_0{}^2}{2\kappa_0^cg_1^s} \quad (10)$$

when the Brillouin lasing output equals to 0. For the cascaded Brillouin lasing, if the last order N^{th} is odd/even number, the odd/even number order Brillouin lasing is relative to $\Delta\omega_0$ as that of even/odd number order lasing is only relative to κ_j^i, κ_j^c and g_j^s. In the following, only single Brillouin lasing is considered.

III. Thermal Perturbations

Two kinds of thermal perturbations on Brillouin lasing are proposed. One is to tune the wavelength of pump wave and the other is to vary the surrounding temperature. When the pump wavelength is manually tuned by a certain value, the resonance will follow the shift of the pump wave as optical resonances are thermally latched by pump wave. The relation between the variation of thermal power ΔP_h and the tuning of pump wavelength $\Delta\lambda_p$ can be briefly expressed as $\Delta P_h=K\Delta\lambda_p/\zeta$,

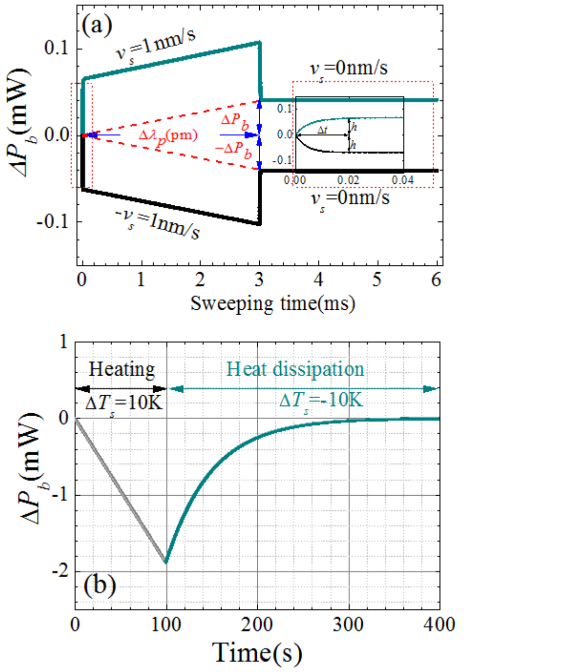

Fig. 2. (a) The variation of the Brillouin microlaser output power ΔP_b as λ_p is swept by 3pm with a speed of v_s=±1nm/s. The inset is the expanded demonstration of dashed rectangle with the same time scale, where the power coupled into taper P_{in}=50mW, κ_0^i/κ_0 or κ_1^i/κ_1=0.2, g_1^s=1.75×10^{14}Hz^2/mW, the thermal capacity of mode area C_m=2.363×10^{-4} mJ/K, K=4.73×10^{-2} mW/K and κ_1 or κ_0=2π×10^{6}Hz, the initial value of Δω= κ_0. (b) ΔP_b depending on time for both heating and heat dissipation processes.

where K is the thermal conductivity between the mode area and the surroundings with unit of W/K, ζ≈13.89pm/K is the thermal coefficient of the wavelength drift of silica, taking into account both the influences from the thermal-induced refractive-index change and cavity expanding[29]. For the single Brillouin lasing, as shown by Eq. (8) and Eq. (9), the relation between the variation of Brillouin lasing output $\Delta P_b = \Delta P_1^c$ and the tuning of pump wave $\Delta\lambda_p$ can thus be constructed as

$$\Delta P_b = \frac{\kappa_1^c}{\kappa_1^i}\frac{K}{\zeta}\Delta\lambda_p \tag{11}$$

the coupling frequency κ_1^c is usually larger than the intrinsic loss κ_1^i for the adhesive coupling of taper, because the coupling loss led by coupling waveguide (without power coupled into cavity) is usually higher than the intrinsic loss of the cavity, which explains why most of Brillouin lasing power can be collected and up to 90% of total power efficiency can be realized[9].

As the pump wavelength λ_p is manually tuned by $\Delta\lambda_p$ whose minimum value is determined by the tuning resolution of pump laser, the total variation of Brillouin lasing output ΔP_b can be obtained from Eq. (11). Fig.2(a) shows the variation of ΔP_b as λ_p is swept by 3pm with a velocity v_s=±1nm/s, which is calculated based on the thermal dynamic equations of microsphere[30]. ΔP_b first jumps by a height of h in a short time of Δt from a thermally steady state to an un-steady state, then linearly increases/decreases following the sweeping of λ_p, and eventually decreases/increases to the secondary steady state with a power jump of h as well. The inset shows the expanded evolution of ΔP_b as λ_p starts sweeping. The jump h is led by the temperature lag of thermal response from the pump wave sweeping due to the fact that the temperature can't jump abruptly, where h is proportional to the sweeping speed v_s while Δt is proportional to input power P_{in}. The over quick sweeping of λ_p generally leads to a great lag of thermal response, if this lag is great enough as the power coupled into cavity is less than the initial value, the resonance λ_r does not shift in red direction, but shift in blue direction and the thermal latching breaks. On the contrary, if the pump is swept in blue direction, the maximum value of jump power h is equivalent to the initial Brillouin lasing output.

As the surrounding temperature T_s is increased/decreased by ΔT_s, the thermal power P_h will decreases/increases by a value of $K\Delta Ts$, and accordingly the variation of Brillouin lasing output ΔP_b can be derived from Eq.(11):

$$\Delta P_b = -\frac{\kappa_1^c}{\kappa_1^i}K\Delta T_s. \tag{12}$$

We assume $T_s=T_{s0}+v_h t$ increases linearly, and $\Delta T_s=T_{s0}+\Delta T_{s0}e^{-t/\tau}$ decreases exponentially, where T_{s0} is the initial temperature, v_h is the temperature increasing speed, and τ is the thermal relax time. In order to mimic the variation in ΔP_b, we set v_h=0.1K/s, τ=50s and the temperature increasing time is 100s, other parameters are the same as those used in Fig.2(a). The results are shown in Fig. 2(b), the lasing output P_b decreases by -1.9mW from the initial value in 100s and then recovers to the initial value as the heater cools down for 300s. P_b follows the change of surrounding temperature T_s and shows no jump. On the other hand, if P_b is tracked by a power meter or oscilloscope, the thermal detection of the surrounding temperature can be realized.

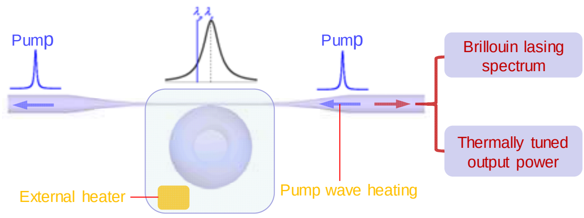

Fig. 3. Schematic illustration of measurement system of Brillouin microsphere laser.

IV. Experimental Demonstrations Of Thermal Perturbations On Brillouin Microsphere Laser

A. Package of microspheres for stable performances of Brillouin lasing

Fig. 3 shows a schematic illustration of the experiment setup for the measurement of microsphere Brillouin lasers. A tunable external cavity laser (TECL) produced by Photonetics Incorporation with the type of Tunics-plus at C band and a typical linewidth of 150kHz is employed as the pump source, the wavelength resolution of TECL is 1pm, and the typical wavelength and power stability are ±3pm/h and ±0.01dB/h,

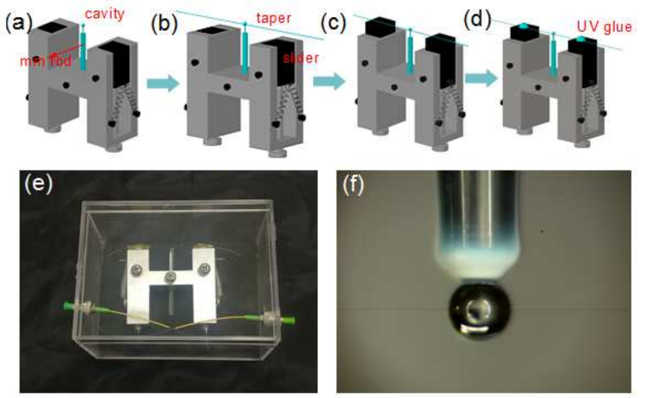

Fig. 4. Packaging steps of the sphere cavity with a fiber taper. (a) A fabricated cavity is firmly fixed by a bolt on a mechanical module; (b) The position of the module with the resonator is tuned by a 3D translation stage to approach to the pulled taper under the monitoring of a microscope. The wide cross section of the sphere cavity allows remarkable coupling tolerance near the equator. (c) The sliders on the module are jacked up to abut against the taper; (d) Ultraviolet(UV) glue is dripped on the top of sliders to fix the taper after several minute solidification. (e) A packaged sphere-taper with two connecting ports. (f) The side view of a sphere cavity coupled with a taper.

respectively. To perform thermal perturbations on the Brillouin laser, sphere cavities fabricated from a 3 millimeter-diameter quartz rod by a mechanical method are employed[31], and a heater, positioned in the box, is used for tuning the temperature of environment. A fiber taper with diameter ranging from 2μm to 4μm, pulled from a single mode fiber, is used to couple the pump wave into the cavity. The power of the backward scattered Brillouin lasing is coupled out by the same taper, then collected by an optical circulator, and subsequently divided into several routes for microlaser diagnosis, for example, using an optical spectrum analyzer (OSA) and a power meter for measuring opitcal spectra and power. In order to track the real-time variation of the laser output, one of routes is coupled into a photodetector, and the real-time variation of power can be monitored by an oscilloscope.

Before the experimental study of thermal characteristics of Brillouin microlasers, a mechanical module is designed and used to package the sphere cavity with a fiber taper in order to stabilize the coupling and achieve stable performances of the Brillouin laser. Detailed packaging steps are presented in Fig. 4(a) to (d). Fig. 4(e) shows a package of the sphere cavity coupled with a fiber taper. Both connectors can be considered as input or output ports for Brillouin lasing. Fig. 4(f) shows the side view of a taper-coupled sphere cavity with a diameter of ~620μm.

The transmission spectrum of the packaged sample is measured and shows typical resonances with Q factors higher than 1×10^8 which are not spoiled due to the packaging. In order to couple the pump wave into cavity, the wavelength of the TECL is manually tuned to latch the pump wave to one of the WGM resonances and the detuning frequency from the coupled resonance $\Delta\omega_0$ is passively chosen. If there exists one resonance located in the Brillouin gain curve, the spontaneous Brillouin scattering will be amplified and transformed into SBS due to longer photon life or higher intensity induced by WGM resonances. The detuning Γ between WGM resonance and Brillouin gain curve is also passively chosen and takes effects on intracavity Brillouin gain g_j^s. In order to present the stability of Brillouin microlaser, three optical spectra of a 5-order cascaded Brillouin lasing with a time interval of 10 minutes are measured and shown in Fig. 5. The highest peak is the 1st-order red-shifted Brillouin lasing while only the backward scattered light is collected. The 1st, 3rd and 5th peaks are the reflected pump wave, the 2nd- and the 4th-order Brillouin lasing, which are resulted from intra-cavity Rayleigh scattering[32][33]. The real time output power is tracked by an oscilloscope as presented in the upper part, the slight decrease of output power is led by the decrease of pump power(amplifier). The inset shows the expanded peak of the 1st-order of Brillouin lasing with a power fluctuation less than 0.2dBm. The results indicate that the coupling strength between the taper and sphere is stable and the mechanical packaging enables stable performances of Brillouin lasing (we also performed measurements on un-packaged spheres in free air, the output is confirmed to be unstable). It means that the coupling noise induced by the displacement of taper and cavity is effectively under control.

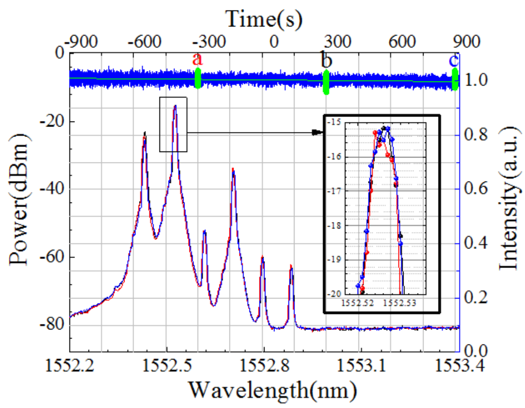

Fig. 5. Three Brillouin lasing spectra recorded in half an hour with time interval of 10 minutes denoted by 'a', 'b' and 'c'. The upper part shows the normalized real time power variation, the slight power decrease(solid line) originates from the slight decrease of pumping power(amplifier). The inset show the expanded optical spectra the 1st–order Brillouin lasing peak.

B. *Wavelength tuning of Pump wave*

To experimentally investigate thermal behaviors of the Brillouin microsphere laser, the pump wavelength λ_p is firstly swept by steps of 10pm over the optical resonances until lasing is realized. The tuning step is then minimized to 1pm. Fig. 6(a) shows a typical variation of lasing output P_b as λ_p is tuned from point 'a' to 'b' and then to 'c' and finally jump to 'd' in a cavity of 620μm. The pump power P_{in} coupled into the taper is ~100mW. The total tuning of ~150pm can be divided into 7 segments denoted by the number from 1 to 7. Fig. 6(b) schematically shows the relative positions of pump λ_p and coupled resonance λ_r of four states denoted by points 'a', 'b', 'c' and 'd'. 'c' and 'd' indicate the nearly complete and incomplete latching states of the pump wave, respectively, while 'a' and 'b' fall in between them. As predicted by Eq.(11), ΔP_b varies linearly with $\Delta\lambda_p$ in all segments from 1 to 7 upon a coefficient κ_1^c/κ_1^i, even though slight noise exists as Rayleigh scattering power is not transferred into thermal power. The power transitions between adjacent segments are led by the resonance transitions of pump wave or Brillouin lasing. As the pump is tuned in red direction from point 'b', more

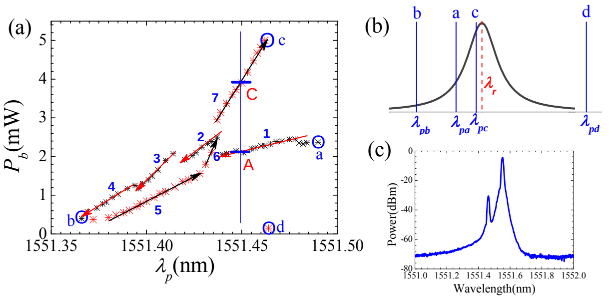

Fig. 6. (a) P_b versus λ_p near 1.55μm as λ_p is firstly tuned from 'a' to 'b' and then tuned back to 'c', and finally to 'd'. (b) The schematic illustration of the relative position of λ_p to λ_r, corresponding to 'a', 'b', 'c' and 'd' points shown in (a). (c) The recorded Brillouin lasing spectrum of 'c'.

power is coupled into cavity and all the WGM resonances(including pump coupled resonance) drift synchronously due to thermal effects(segment 5). If the pump power coupled into cavity P_c increases to the maximum value for the coupled resonance, namely λ_p-λ_r≈0 or $\Delta\omega_0$=0, the thermal power P_h can't support the resonance shift as the pump λ_p is further tuned(transition between 5 and 6), and the thermal latching breaks. The pump power P_c coupled into cavity decreases to zero and the resonances start to shift in blue direction during the process of heat dissipation until another resonance latches again. The newly coupled resonance should have greater coupling frequency κ_0^c (seen from Eq.(9)), otherwise thermal power still cannot support the already induced resonance shift(assume a slight blue shift occurs as the latching transits from one resonance to another). The above mentioned process repeats for the newly coupled pump wave(segment 6), and if there is no resonance to get a higher κ_0^c, the latching completely breaks and finally P_c decreases to 0(point 'd'). On the contrary, if the pump λ_p is tuned in blue direction(segment 1), the thermal power P_h decreases and the resonances λ_r drift to the shorter wavelength. The output transitions between segments 1 and 2 or others cannot be attributed to the resonance transitions of pump wave, it is because only when P_h decreases to zero, the transition can happen as the pump λ_p is further tuned. Thus, we attribute the hopping of the output to the lasing transition between different resonances as λ_p is tuned in blue direction, because the band width of the Brillouin gain spectrum is a few tens of megahertz which may cover several resonances of large sphere cavities (this can be confirmed by the measured transmission spectrum), and the lasing competition between resonances may exist due to the dispersion of resonance shift. In Fig. 6(c), the Brillouin lasing spectrum at point 'c' is presented.

The optical bistabilities due to the resonance transition of pump wave or Brillouin lasing are quite universally observed in large cavities with intense resonances. Obviously, the detuning wavelength λ_r-λ_p between resonance and pump wave is different at 'C' and 'A' states. If the pump coupled resonances are the same one at 'C' and 'A', the resonance wavelength λ_r should be the same as λ_r is latched by the same λ_p, the thermal power P_h should be the same as well. However, as shown by Eq.(8) and Eq.(9), P_h should be different as the lasing output P_b is different, it is inconsistent with the assumption of the same coupled resonance of pump wave. Thus the resonances transition of

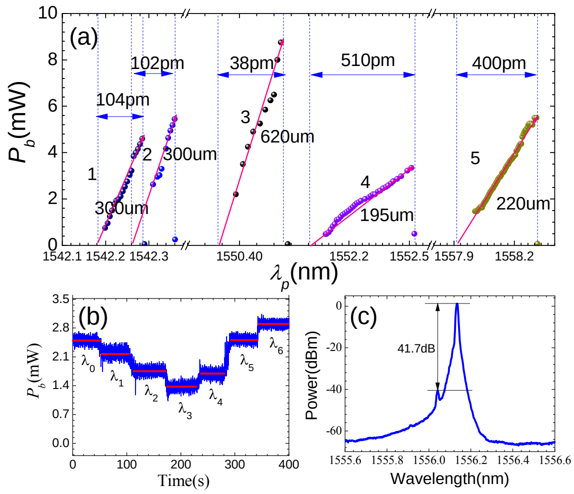

Fig. 7. (a) P_b versus λ_p in samples with diameters ranging from ~200μm to ~600μm. (b) The power evolution recorded by an oscilloscope as λ_p is tuned in a ~300um-diameter cavity. (c) A Brillouin lasing spectrum with a SMSR of 41.7 dB.

pump wave certainly exists and optical bistabilities are attributed to the resonance transitions of pump wave and Brillouin lasing with different κ_1^i, κ_1^c and g_1^s.

In the following, we give five typical results from four samples with diameters ranged from ~200μm to ~600μm, including two results from a ~300μm-diameter cavity. As shown in Fig. 7 (a), where we estimate the total tuning bandwidth Λ_w by extrapolating the lasing output P_b to zero, since we cannot fully tune the pump λ_p as λ_p is randomly latched to one of WGMs. Λ_w is 104pm and 102pm for the 300μm-diameter cavity, and 38pm, 510pm and 400pm for cavities with diameters of ~620μm, ~195μm and ~220μm, respectively. Smaller cavities usually accommodate greater Λ_w, due to the smaller heat conductivity K. For the same cavity, Λ_w varies from mode to mode, the thermal power P_h or Brillouin lasing output P_b is accordingly different. In addition, different P_b also leads to different P_h and Λ_w. Fig. 7 (b) shows a real-time P_b tracked by an oscilloscope for back and forth tuning in a 300 μm-diameter sphere. The pump wavelength λ_p is first tuned from λ_0 to λ_3 in the blue direction, and then tuned back to λ_6. Here, the tuning interval keeps 10pm except that λ_5-λ_4=25pm. The lasing outputs are estimated to be 2.50, 2.17, 1.75, 1.38, 1.70, 2.51 and 2.90mW respectively. The temperature sensitivity of the mode region is thus between 0.444mW/K and 0.584mW/K. Generally speaking, Brillouin lasing in larger cavities has greater sensitivities than that of smaller cavities for the same thermal power P_h, while it is mainly determined by the total lasing power conversion efficiency. For example, P_h is usually lower and Λ_w is smaller for a great lasing output. As shown in Fig. 7(c), we give a spectrum from a ~300μm-diameter Brillouin laser, where the lasing output is ~26.2mW and the total power conversion efficiency is estimated to be 67%~87%. Therefore, the thermal sensitivity is greater than 3.64mW/K (0.262mW/pm) as total tuning bandwidth Λ_w is less than 100pm for a smaller thermal power P_h. The demonstrated 41.7dB of SMSR, to the best of our knowledge, is the highest reported value to date in WGM Brillouin microlasers.

C. Temperature variations of surroundings

The thermal influence on Brillouin microlaser induced by temperature variations of surroundings is also studied. Firstly, the system is heated up to a certain temperature $T_s+\Delta T$ (T_s is the room temperature). When heating stops, the lasing output is recorded within a few minutes as the thermal power is dissipated from the heater into air and the temperature of the cavity decreases accordingly. Finally, the heater is operated again with different heating-up speeds and time. As shown in Fig. 8, the measured results are fitted by setting proper parameters. The thermal sensitivity of Brillouin lasing on the surrounding temperature is estimated to be within the range from 0.51mW/K to 0.55 mW/K, close to the values of that in mode area. The results indicate that the Brillouin lasing output can be linearly tuned by increasing or decreasing the temperature of surroundings, which hold great potential for the application of thermal sensing.

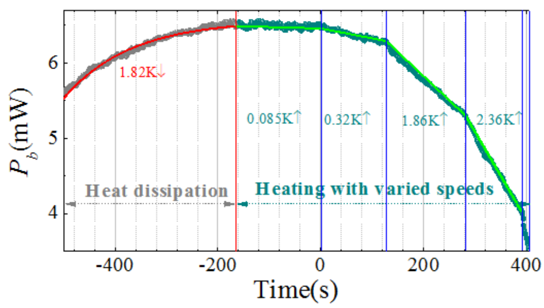

Fig. 8. Brillouin lasing output versus thermal tuning time. Both heat dissipation and heating processes are considered.

V. Conclusion

In conclusion, the thermal characteristics of Brillouin silica microsphere lasers have been investigated. The constructed analytic model based on couple mode theory predicts that the output power of Brillouin lasing will linearly vary with the resonant shift induced by the thermal perturbations. In order to verify the theoretical prediction, mechanically packaged microspheres are employed and experiments are simply performed by either tuning the wavelength of pump wave or varying the environmental temperatures. The results clearly confirm our theoretical prediction. Optical bistabilities induced by the resonant transition of pump wave or Brillouin lasing, are demonstrated and well explained by thermal dynamics of microcavities. On the other hand, by simply tracking the output power of Brillouin laser, we can detect the temperature change of environments resulting in the shift of microsphere resonances, which demonstrates the potential application of Brillouin microsphere lasers for thermal sensors. Except thermal perturbation, optical perturbations on evanescent wave, such as adherence of biomolecules and optical coupling from a probe light, can also be detected from the variation of Brillouin lasing output power.

References

[1] R. Chiao, C. Townes, and B. Stoicheff, "Stimulated Brillouin scattering and coherent generation of intense hypersonic waves," *Phys. Rev. Lett.*, vol.12, no.21 pp.592-595, 1964.

[2] E. Ippen and R. Stolen, "Stimulated Brillouin scattering in optical fibers," *Appl. Phys. Lett.*, vol.**21**, no.11, pp.539-541, 1972.

[3] A. Kobyakov, M. Sauer, and D. Chowdhury, "Stimulated Brillouin scattering in optical fibers," *Adv. Opt. Photonics*, vol. 2, pp.1-59, 2010.

[4] Elsa Garmire, "Perspectives on stimulated Brillouin scattering," *New J. Phys.*, vol. 19, pp. 011003, 2017.

[5] R. Pant, C. G. Poulton, D. Y. Choi, H. Mcfarlane, S. Hile, E. Li, L. Thevenaz, B. L. Davies, S. J. Madden, and B. J. Eggleton, Opt. Express, **19**, 8285(2011).

[6] B. Morrison, A. Casas-bedoya, G. H. Ren, K. Vu, Y. Liu, A, Zarifi, T. G. Nguyen,D. Y. Choi, D. Marpaung, S. J. Madden, A. Mitchell and B. J. Eggleton, "Compact Brillouin devices through hybrid integration on silicon *Optica*, vol. **4**, no.8, pp.847-854, 2017.

[7] H. Shin, W. J. Qiu, R. Jarecki, J.n A. Cox, R. H. Olsson III, A. Starbuck, Z. Wang & P. T. Rakich, "Tailorable stimulated Brillouin scattering in nanoscale silicon waveguides," *Nat. Commun.*, 4(1944), pp.1-10, 2013.

[8] J. Z. Zhang, R. K. Chang, "Generation and suppression of stimulated Brillouin scattering in single liquid droplets," *J. Opt. Soc. Amer. B*, vol. 6, no.2, pp.151-153, 1988.

[9] I. S. Grudinin, A. B. Matsko, and L. Maleki, "Brillouin Lasing with a CaF_2 Whispering Gallery Mode Resonator," *Phys. Rev. Lett.*, vol.102, pp. 043902, 2009.

[10] M. Tomes and T. Carmon, "Photonic Micro-Electromechanical Systems Vibrating at X-band (11-GHz) Rates," *Phys. Rev. Lett.*, vol. 102, pp.113601, 2009.

[11] G. Bahl, J. Zehnpfennig, M. Tomes & T. Carmon, "Stimulated optomechanical excitation of surface acoustic waves in a microdevice," *Nature Commun.*, vol. 2, pp.403, 2011.

[12] C. L. Guo, K. J. Che, Z. P. Cai, S. Liu, G. Q. Gu, C. X. Chu, P. Zhang, H. Y. Fu, Z. Q. Luo, and H. Y. Xu, "Ultralow-threshold cascaded Brillouin microlaser for tunable microwave generation," *Opt. Lett.*, vol.40, no.21, pp.4971-4974, 2015.

[13] K. J. Che, P. Zhang, C. L. Guo, D. Y. Tang, C. Y. Ren, H. Y. Xu, Z. Q. Luo, Z. P. Cai, "Ultra-high Q sphere-like cavities for cascaded stimulated Brillouin lasing," *Opt. Comm.*, vol. 387, pp. 421-425, 2017.

[14] C. L. Guo, K. J. Che, P. Zhang, J. S. Wu, Y. T. Huang, H.Y. Xu, and Z. P. Cai, "Low-threshold stimulated Brillouin scattering in high-Q whispering gallery mode tellurite microspheres," *Opt. Express*, vol. 23**,** no.25, pp. 32261, 2015.

[15] P. Del'Haye, S. A. Diddams, and S. B. Papp, "Laser-machined ultra-high-Q microrod resonators for nonlinear optics," *Appl. Phys. Lett.*, vol. 102, pp. 221119, 2013.

[16] M. Asano, Y. Takeuchi, S. K. Ozdemir, R. Ikuta, L. Yang, N. Imoto,1 and T. Yamamoto, "Stimulated Brillouin scattering and Brillouin-coupled four-wave-mixing in a silica microbottle resonator," *Opt. Express*, vol.24, no. 11, pp.12082-12092, 2016.

[17] Q. J. Lu, S. Liu, X. Wu, L. Y. Liu, and L. Xu, "Stimulated Brillouin laser and frequency comb generation in high-Q microbubble resonators," *Opt. Lett.*, vol. 41, no.8, pp.1736-1739, 2016.

[18] A. A. Savchenkov, A. B. Matsko, V. S. Ilchenko, D. Seidel, and L. Maleki, "Surface acoustic wave opto-mechanical oscillator and frequency comb generator," *Opt. Lett.*, vol.36, no.19, pp. 3338-3340, 2011.

[19] G. P. Lin, S. Diallo, K. Saleh, R. Martinenghi, J. C. Beugnot, T. Sylvestre, and Y. K. Chembo, "Cascaded Brillouin lasing in monolithic barium fluoride whispering gallery mode resonators," *Appl. Phys. Lett.*, vol. 105, pp. 231103, 2014.

[20] H. Lee, T. Chen, J. Li, K. Y. Yang, S. Jeon, O. Painter and K. J. Vahala, Nature photon., "Chemically etched ultrahigh-Q wedge-resonator on a silicon chip," vol. 6, pp. 369-373, 2012.

[21] J. Li, H. Lee & K. J. Vahala, "Microwave synthesizer using an on-chip Brillouin oscillator," *Nat. Commun.*, vol. 4, pp. 2097, 2013.

[22] A. Choudhary, I. Aryanfar, S. Shahnia, B. Morrison, K. Vu, S. Madden, B. Lutner-davies, D. Marpaung and B. J. Eggleton, "Tailoring of the Brillouin gain for on-chip widely tunable and reconfigurable broadband microwave photonic filters," *Opt. Lett.*, vol. 41, no.3 pp.436-439, 2016.

[23] C. H. Dong, Z. Shen, C. L. Zou, Y. L. Zhang, W. Fu & G. C. Guo, "Brillouin-scattering-induced transparency and non-reciprocal light storage," *Nat. Commun.*, vol. 6, pp. 6193, 2015.

[24] J. Kim, M. C. Kuzyk, K. Han, H. Wang and G. Bahl, "Non-reciprocal Brillouin scattering induced transparency," *Nature Phys.*, vol. 11, pp. 275-280, 2015.

[25] J. Li, M. G. Suh, and K. J. Vahala, "Microresonator Brillouin gyroscope," *Optica*, vol. **4**, no.3 pp.346-348, 2017.

[26] A. Chiasera, Y. Dumeige, P. Feron, M. Ferrari, Y. Jestin, G. N. Conti, S. Pelli, S. Soria, and G. C. Righini, "Spherical whispering-gallery-mode microresonators," *Laser Photon. Rev.*, vol. 4, no.3, pp.457-482, 2010.

[27] B. E. Little, S. T. Chu, H. A. Haus, J. Foresi, and J. P. Laine, "Microring Resonator Channel Dropping Filters," *J. Lightwave Technol.*, vol. 15, pp. 998–1005, 1997.

[28] B. Min, T. J. Kippenberg, and K. J. Vahala, "Compact, fiber-compatible, cascaded Raman laser," *Opt. Lett.,* vol. 28, no.17, pp.1507-1509, 2003.

[29] Q. Ma, T. Rossmann and Z. Guo, "Temperature sensitivity of silica micro-resonators," *J. Phys. D: Appl. Phys.* vol. 41, pp. 245111, 2008.

[30] T. Carmon, L. Yang, and K. J. Vahala, "Dynamical thermal behavior and thermal self-stability of microcavities," *Opt. Express,* vol. **12**, no.20, pp. 4742-4750, 2004.

[31] K. J. Che, P. Zhang, C. L. Guo, D. Y. Tang, C. Y. Ren, H. Y. Xu, Z. Q. Luo, Z. P. Cai, "Ultra-high Q sphere-like cavities for cascaded stimulated Brillouin lasing," *Opt. Comm.*, vol. 387, pp. 421-425, 2017.

[32] M. L. Gorodetsky, A. D. Pryamikov, V. S. Ilchenko, "Rayleigh scattering in high-Q microspheres," *J. Opt. Soc. Amer. B*, vol.17, no.6, pp.1051-1057, 2000.

[33] T. J. Kippenberg, S. M. Spillane, and K. J. Vahala, "Modal coupling in traveling-wave resonators," *Opt. Lett.,* vol. 27, no.19, pp.1669-1671, 2002.